Supporting Information

Efficient Co-Upcycling of Glycerol and CO₂ into Valuable Products Enabled by a Bifunctional Ru-Complex Catalyst

Tianhua Cui,[†, a] Huihua Gong,[†, b] Li Ji,[c] Jiawei Mao,[d] Weichao Xue,[a] Xueli Zheng,[a] Haiyan Fu,[a] Hua Chen,[a] Ruixiang Li,[*, a] and Jiaqi Xu[*, a, e]

a. Key Laboratory of Green Chemistry and Technology of Ministry of Education, College of Chemistry, Sichuan University, Chengdu, Sichuan 610064, China.

b. Analytical and Testing Center, College of Chemistry and Chemical Engineering, Neijiang Normal University, Neijiang 641112, P. R. China

c. Sichuan Research Institute of Chemical Quality and Safety Testing, Chengdu, Sichuan 610031, P.R. China

d. Sichuan Institute of Product Quality Supervision and Inspection, Chengdu, Sichuan 610100, P.R. China

e. Laboratory of Photonics and Interfaces, École Polytechnique Fédérale de Lausanne, 1015 Lausanne, Switzerland

* Email: liruixiang@scu.edu.cn, jqxu@scu.edu.cn

[†] These authors contributed equally to this work.

[‡] Dedicated to Prof. Michael Grätzel on the occasion of his 80th birthday.

1. Experimental procedure

FTIR and *in-situ* FTIR measurements:

FTIR spectra were recorded with a Nicolet iS50 spectrometer equipped with an MCT detector. The complex **2** was ground into a powder and placed into sample cells. A liquid film was formed by dripping an aqueous solution of glycerol and K_2CO_3 onto the catalyst powder. After purging with CO_2 for half an hour, the background spectrum was measured by heating to 90 °C under a CO_2 atmosphere. The *in-situ* FTIR measurements were monitored in real-time with a time resolution of 10 min per spectrum at 90 °C.

Calculations of TONs and TOFs:

$$TON_{formate} = \frac{n_{formate}}{n_{cat}}$$

$$TON_{lactate} = \frac{n_{lactate}}{n_{cat}}$$

$$TOF_{formate} = \frac{TON_{formate}}{t}$$

$$TOF_{lactate} = \frac{TON_{lactate}}{t}$$

Standard procedures for the upcycling of CO_2 and glycerol and catalyst stability test.

Standard procedure: After water and glycerol (5 mL/5 mL) were mixed and degassed, the degassed solution, catalyst (0.1 μmol) and base (24 mmol) were added into the autoclave with a magnetic stirrer, and then the autoclave was closed and flushed with CO_2 for 3 times. Subsequently, after the autoclave was pressured to the designed pressure with CO_2, it was heated to the desired temperature, the stirrer was turned on and the reaction was performed for 20 hours. At the end of the reaction, the autoclave was cooled to room temperature, then 0.5 mL of D_2O and DMF as an internal standard were added to the reaction mixture for ^{1}H NMR analysis.

Catalyst stability test: Under standard reaction conditions, the reaction temperature is maintained at 200 °C. Stirring is paused at 5, 20, 50, and 100 hours. A small amount of reaction liquid is then extracted from the reactor using internal pressure for ^{1}H NMR analysis.

Degassing method:

After the reaction solution was added into a round-bottom flask, it was sealed and connected with the vacuum line. Subsequently, the flask was immersed in liquid nitrogen until the solution was frozen completely. The frozen mixture solution was pumped to vacuum for 5 min, after which the flask was flushed with nitrogen and the solution was allowed to thaw. The freeze-thaw cycle was performed 3 times. After the final cycle, the solution was allowed to thaw completely at room temperature. The degassed solvent was then transferred to the reaction vessel using a syringe with a long needle under a N_2 atmosphere.
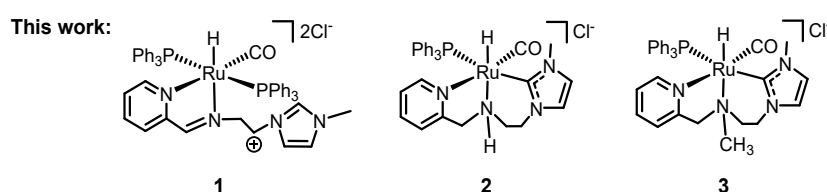
Scheme S1. Ru complexes for co-upcycling of CO_2 and glycerol.

1.1 Synthesis and characterization of complex
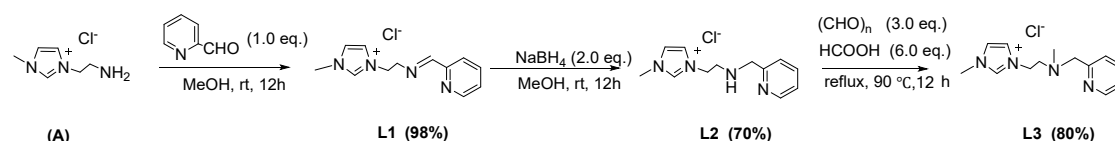
Scheme S2. Synthesis of ligand **L1, L2, L3**.

The Ru-CNN complexes **1**, **2** and **3** were prepared according to previous reports with small modification[1].

Synthesis of 1-methyl-3-{2-{(pyridin-2-ylmethylene)-imino}-ethyl}-1H-imidazol-3-ium Chloride (ligand L1, CN^{im}N): A mixture of 2-chloroethylamine hydrochloride and 1-methylimidazole (2.0 eq.) was stirred in dried acetonitrile at 90 °C for 12 h. The precipitate was filtered, washed with EtOH, and then dried in vacuo to give the hydrochloride of (**A**) as a white solid (85%). After the white solid was dissolved in minimal water, the pH value of the aqueous solution was adjusted to 8-9 with KOH solution and stirred for 30 minutes. Subsequently, all water was removed by rotary evaporation and the residue was extracted by the mixture solution of THF/EtOH (1:4, 50mL). The extraction solution was collected and the solvent was removed under

reduced pressure to give the desired product (**A**) as a pale-yellow liquid. Product **A** (1.616g, 10 mmol) was dissolved in 30 mL anhydrous methanol, and pyridine-2-carboxaldehyde (1.071g, 10 mmol) was added to the solution followed by stirring the mixture at room temperature for 12 h. And then the solvent was removed in vacuo to yield the product as brownish yellow solid (2.5 g, 98%). ^1H NMR (400 MHz, DMSO-d_6, δ): 9.19 (s, 1H), 8.65 (m, 1H), 8.34 (s, 1H), 7.97 (dt, J = 7.9 Hz, 1.2 Hz, 1H), 7.90 (td, J = 7.7, 1.8 Hz, 1H), 7.79 (t, J = 1.8 Hz, 1H), 7.70 (t, J = 1.8 Hz, 1H), 7.49 (m, 1H), 4.54 (t, J =6.0 Hz, 2H), 4.04 (t, J = 5.6 Hz, 2H), 3.85 (s, 3H). ^{13}C NMR (100 MHz, DMSO-d_6, δ): 165.0, 154.1, 149.9, 137.5, 125.9, 123.9, 123.1, 121.2, 59.1, 50.0, 36.2. HRMS (ESI-TOF) m/z: [M-Cl]$^+$ calcd for $C_{12}H_{15}N_4^+$, 215.1297, found 215.1275.

Synthesis of 1-methyl-3-{2-{(pyridin-2-ylmethyl)-amino}-ethyl}-1H-imidazol-3-ium Chloride (ligand L2, CN^{H}N): NaBH$_4$ (0.379 g, 10 mmol) was added to a round bottom flask, and then methanol solution of ligand **L1** (2.500g, 10 mmol) was added in it cooled with an ice-water bath. This mixture solution was stirred at room temperature for 12 h. At the end of the reaction, the reaction was quenched with 10% HCl aqueous solution. The pH of the resulting aqueous solution was adjusted to 7 with saturated aqueous NaHCO$_3$. All solvents were removed by rotary evaporation and residue was extracted with CH$_2$Cl$_2$. The extraction solution was purified by column chromatography {200-300 mesh silica gel, dichloromethane/ethanol (10:1), Rf = 0.3} to give ligand **L2** as a pale yellow solid (1.76 g, 70%). ^1H NMR (400 MHz, DMSO-d_6, δ): 9.19 (s, 1H), 8.49 (m, 1H), 7.77 (t, J = 1.8 Hz, 1H), 7.74 (dd, J = 7.7, 1.8 Hz, 1H), 7.70 (t, J = 1.8 Hz, 1H), 7.35 (d, J = 7.7 Hz, 1H), 7.25 (m, 1H), 4.26 (t, J = 5.7 Hz, 2H), 3.87 (s, 3H), 3.80 (s, 2H), 2.91 (t, 1H, J =5.7 Hz, 2H). ^{13}C NMR (100 MHz, DMSO-d_6, δ): 160.2, 149.2, 137.4, 137.0, 123.7, 123.1, 122.5, 122.3, 54.1, 49.0, 48.3, 36.2. HRMS (ESI-TOF) m/z: [M-Cl]$^+$ calcd for $C_{12}H_{17}N_4^+$, 217.1453, found 217.1450.

Synthesis of 1-methyl-3-{2-{methyl(pyridin-2-ylmethyl)-amino}-ethyl}-1H-imidazol-3-ium Chloride (ligand L3, CN^{Me}N): A mixture of ligand **L2** (801 mg, 3.18 mmol), paraformaldehyde (286.2 mg, 9.54 mmol) and formic acid (878.7 mg, 0.72 mL, 19.09 mmol) was stirred at 110 °C for 12 h, and then a saturated Na$_2$CO$_3$ solution was added in it until the solution became the alkaline. The resulting mixture was vigorously stirred for 2 h at 110 °C and solvent was removed by rotary

evaporation. The residue was extracted with CH_2Cl_2, and the CH_2Cl_2 solution was evaporated under vacuum to give ligand **L3** as a yellow brown oil. (677 mg, 80%). ^1H NMR (400 MHz, DMSO-d_6, δ): 9.38 (s, 1H), 8.47 (m, 1H), 7.78 (t, J = 1.8 Hz, 1H), 7.76-7.67 (m, 2H), 7.25 (m, 1H), 7.13 (d, J = 7.8 Hz, 1H), 4.35 (t, J=5.7 Hz, 2H), 3.91 (s, 3H), 3.65 (s, 2H), 2.79 (t, J=5.7 Hz, 2H), 2.25 (s, 3H). ^{13}C NMR (100 MHz, DMSO-d_6, δ): 158.9, 149.2, 137.4, 137.0, 123.5, 123.1, 123.1, 122.7, 63.0, 56.1, 47.0, 42.3, 36.2. HRMS (ESI-TOF) m/z: [M-Cl]$^+$ calcd for $C_{13}H_{19}N_4^+$, 231.1610, found 231.1602.

Synthesis of complex $[RuH(CO)(PPh_3)_2(\kappa^2\text{-}CN^{im}N)](Cl)_2$ **(1):** Ligand **L1** (0.25 mmol, 62.5 mg) and $RuHCl(CO)(PPh_3)_3$ (0.25 mmol, 238 mg) were added to a 60 mL mixed solvent of methanol and toluene (1:3) in a two-necked flask under argon atmosphere, and the mixture was stirred at room temperature for 10 h. At the end of the reaction, the solution was concentrated to about 15 mL and 20 ml of ether was added into it to precipitate the desired complex. Subsequently, the precipitate was filtered, washed three times with ether and dried under vacuum to give complex **1** as a bright yellow solid (235 mg, 0.2 mmol, 80%). ^1H NMR (DMSO-d_6, 400 MHz, δ): 9.43 (s, 1H), 8.96 (s, 1H), 7.77 (m, 5H), 7.39 (m, 30H), 6.65 (t, J = 6.6 Hz, 1H), 4.06 (m, 4H), 3.92 (s, 3H), -11.23 (t, J = 20.2 Hz, 1H). $^{31}P\{^1H\}$ NMR (DMSO-d_6, 162 MHz, δ): 44.3 (s). HRMS (ESI-TOF) m/z: [M-2Cl]$^{2+}$ calcd for $C_{49}H_{46}N_4OP_2Ru$, 435.1095, found 435.1093. IR (KBr Disc, cm^{-1}): 1942 (CO).

Synthesis of complex $[fac\text{-}RuH(CO)(PPh_3)\text{-}(\kappa^3\text{-}CN^HN)]Cl$ **(2):** (Method one) Ligand **L2** (0.4 mmol, 100.8 mg), $RuHCl(CO)(PPh_3)_3$ (0.4 mmol, 381 mg) and $NaBH_4$ (0.80 mmol, 30.26 mg) was added to a 60 mL mixed solvent of methanol and toluene in a two-necked flask under argon atmosphere. After the mixture was stirred at 90 °C for 48 h, the solvent was removed in vacuum and then extracted with dehydrated dichloromethane. The volume of dichloromethane solution was concentrated to about 5 mL, and then added with 10 ml of ether to precipitate product. The precipitate was filtered, washed three times with ether and dried under vacuum to give complex **2** as a reddish brown solid (142 mg, 0.22 mmol, 55%). The product is stable to ambient atmosphere in the solid state, and is easy to absorb water in the air. Method two: complex **2** was prepared in a manner analogous to method one except of using CH_3CH_2ONa (1.2 eq.) as base and mixture of ethanol and toluene as the solvent. ^1H NMR (400 MHz, DMSO-d_6, δ): 7.94 (d, J = 5.5 Hz, 1H), 7.66

(t, J = 7.7 Hz, 1H), 7.43-7.26 (m, 18H), 6.86 (t, J = 6.6 Hz, 1H), 5.64 (brs, 1H), 4.18-3.93 (m, 5H), 3.90-3.77 (m, 1H), 3.74-3.54 (m, 2H), 2.42-2.28 (m, 1H), -12.11 (d, J = 25.1 Hz, 1H). ^{31}P{^{1}H} NMR (DMSO-d_6, 162 MHz, δ): 48.0 (s). ^{13}C NMR (100 MHz, DMSO-d_6, δ): 206.2 (d, J = 14.7 Hz, CO), 179.0 (d, J = 87.6 Hz, NHC carbon atom), 159.7, 154.2, 138.2, 135.2 (d, J = 37.3 Hz), 133.2 (d, J = 11.1 Hz), 130.1, 129.0 (d, J = 9.0 Hz), 124.9, 123.0, 122.5, 58.9, 52.6, 48.7, 38.9. HRMS (ESI-TOF) m/z: [M-Cl]$^{+}$ calcd for $C_{31}H_{32}N_4OPRu$, 609.1357; found, 609.1360. IR (KBr Disc, cm^{-1}): 1923 (CO).

Synthesis of complex [fac-RuH(CO)(PPh$_3$)-(κ^3-CN^{Me}N)]Cl **(3):** Complex **3** was prepared with RuHCl(CO)(PPh$_3$)$_3$ and Ligand **L3** by a analogous manner to complex **2** except of using CH$_3$CH$_2$ONa (1.2 eq.) as base and mixture of ethanol and toluene as the solvent (pale white solid, 50%). ^{1}H NMR (DMSO-d_6, 400 MHz, δ): 7.92 (d, J = 5.4 Hz, 1H), 7.72 (t, J = 7.7 Hz, 1H), 7.45-7.28 (m, 18H), 6.89 (t, J = 6.5 Hz, 1H), 4.15 (dd, J = 15.4, 7.9 Hz, 1H), 4.06 (s, 3H), 3.98 (d, J = 15.8 Hz, 1H), 3.78 (dd, J = 15.3, 7.2 Hz, 1H), 3.68 (d, J = 15.8 Hz, 1H), 2.93 (dd, J = 13.4, 7.3 Hz, 1H), 2.74 (s, 3H), 2.56 (dd, J = 13.4, 7.9 Hz, 1H), -13.31 (d, J = 26.9 Hz, 1H). ^{31}P{^{1}H} NMR (DMSO-d_6, 162 MHz, δ): 44.9 (s). ^{13}C NMR (100 MHz, DMSO-d_6, δ): 206.3 (d, J = 15.3 Hz, CO), 178.2 (d, J = 86.7 Hz, NHC carbon atom), 159.5 , 154.1 , 138.6 , 135.7 (d, J = 36.7 Hz), 133.4 (d, J = 10.5 Hz), 130.1, 128.9 (d, J = 8.6 Hz), 125.0, 123.1, 123.0, 122.9, 68.6, 63.0, 53.5, 47.0, 39.2. HRMS (ESI-TOF) m/z: [M-Cl]$^{+}$ calcd for $C_{32}H_{34}N_4OPRu$, 623.1514, found, 623.1466. IR (KBr Disc, cm^{-1}): 1918 (CO).
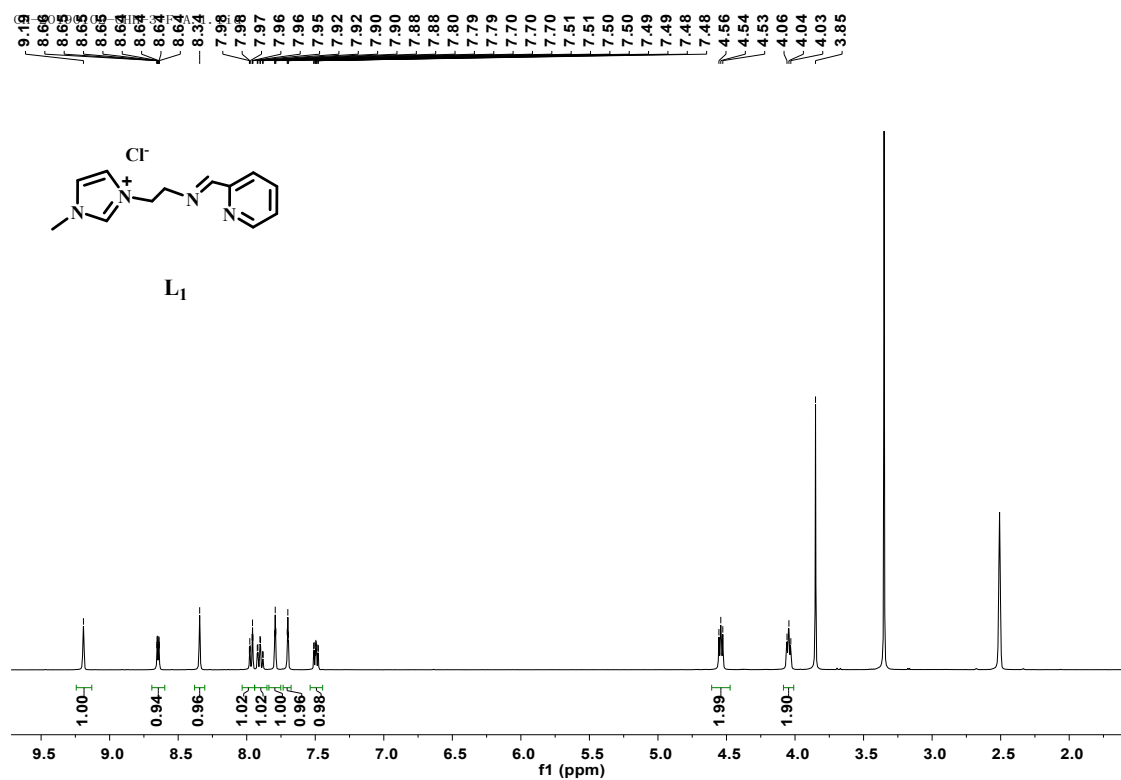
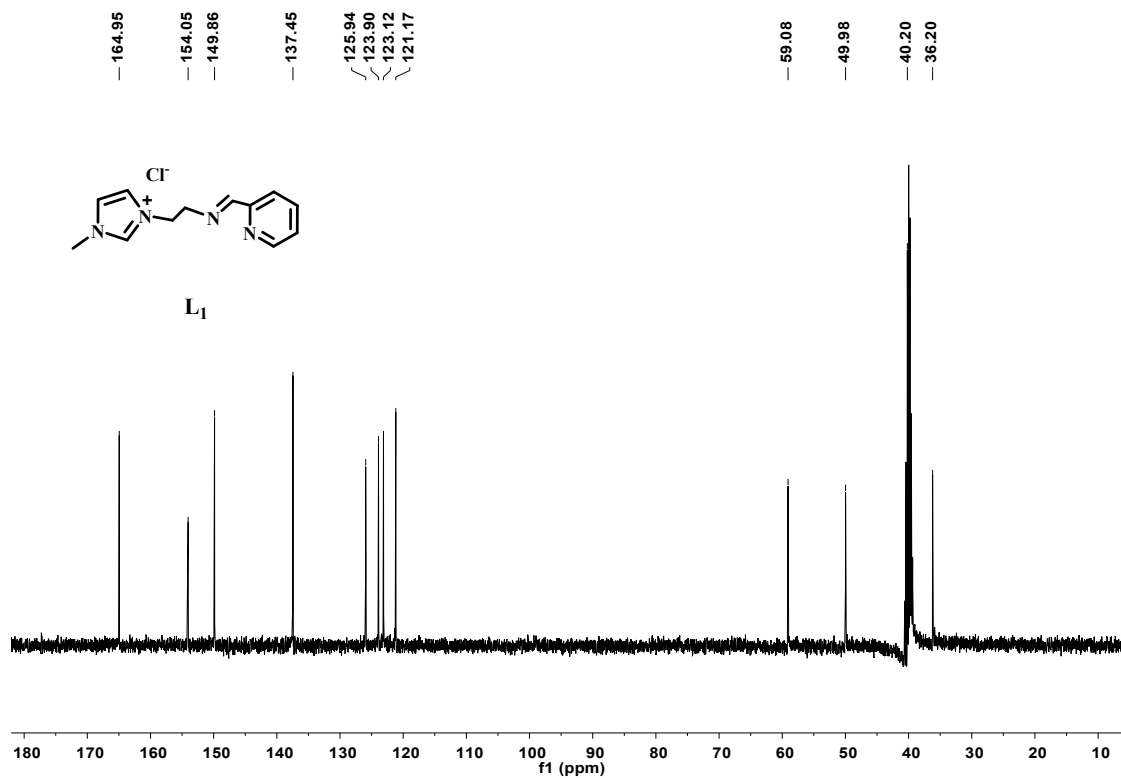**Figure S1**. ^{1}H NMR spectrum of **L1** (400 MHz, DMSO-d_6).

Figure S2. ^{13}C NMR spectrum of **L1** (100 MHz, DMSO-d_6).
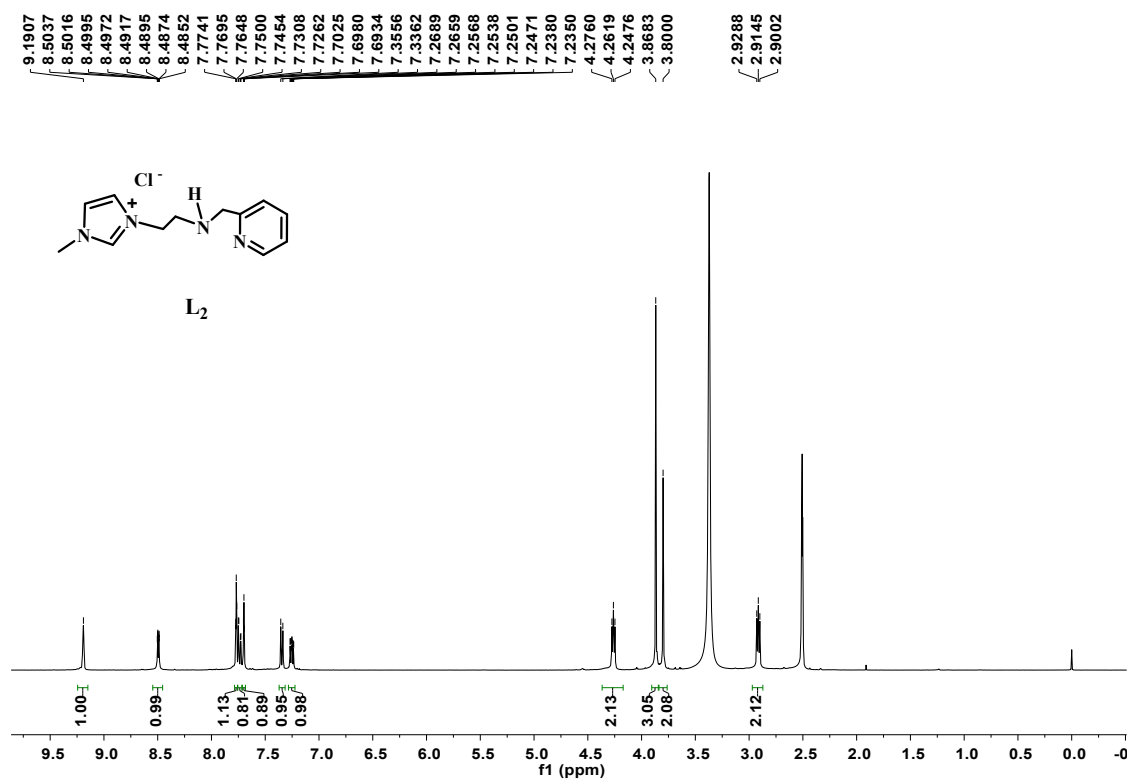
Figure S3. ^{1}H NMR spectrum of **L2** (400 MHz, DMSO-d_6).
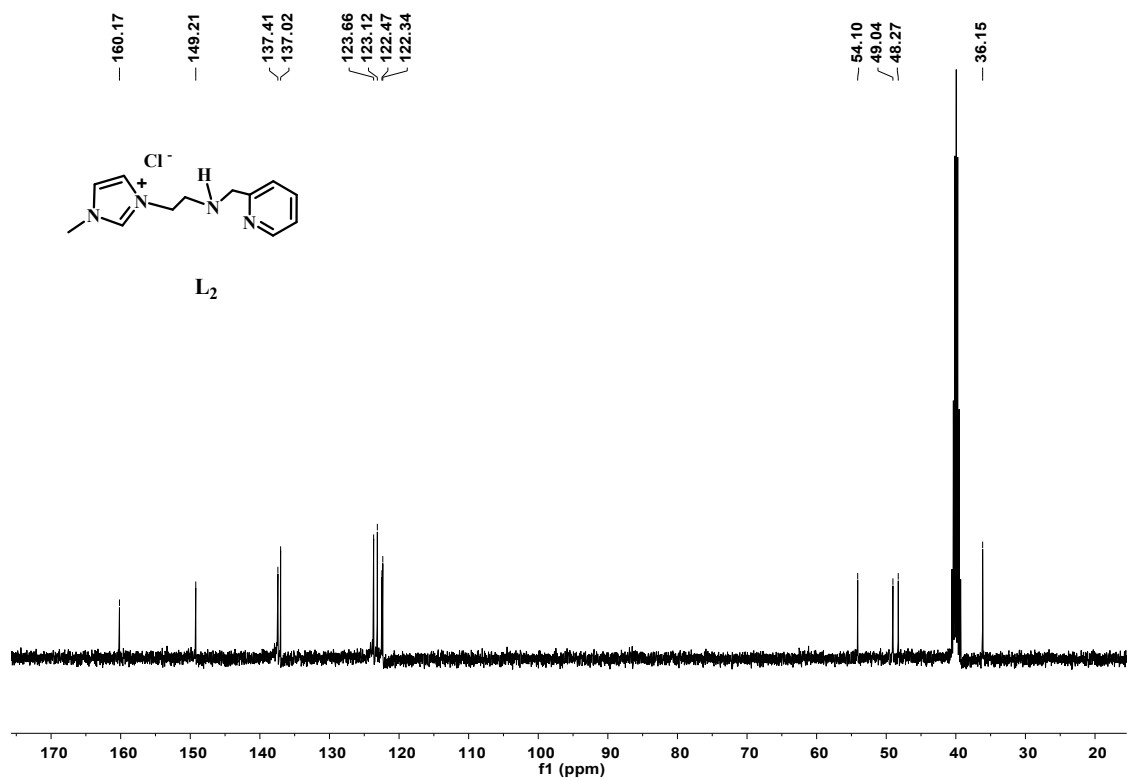
Figure S4. ^{13}C NMR spectrum of **L2** (100 MHz, DMSO-d_6).
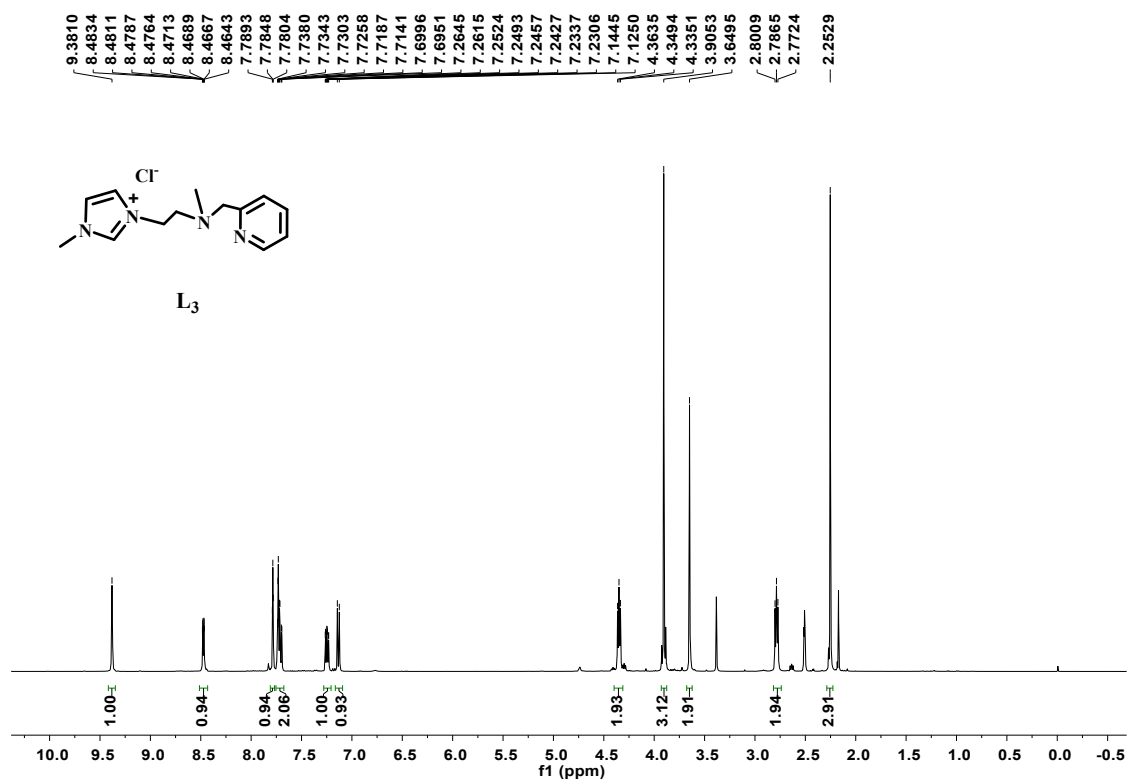
Figure S5. ^1H NMR spectrum of **L3** (400 MHz, DMSO-d_6).
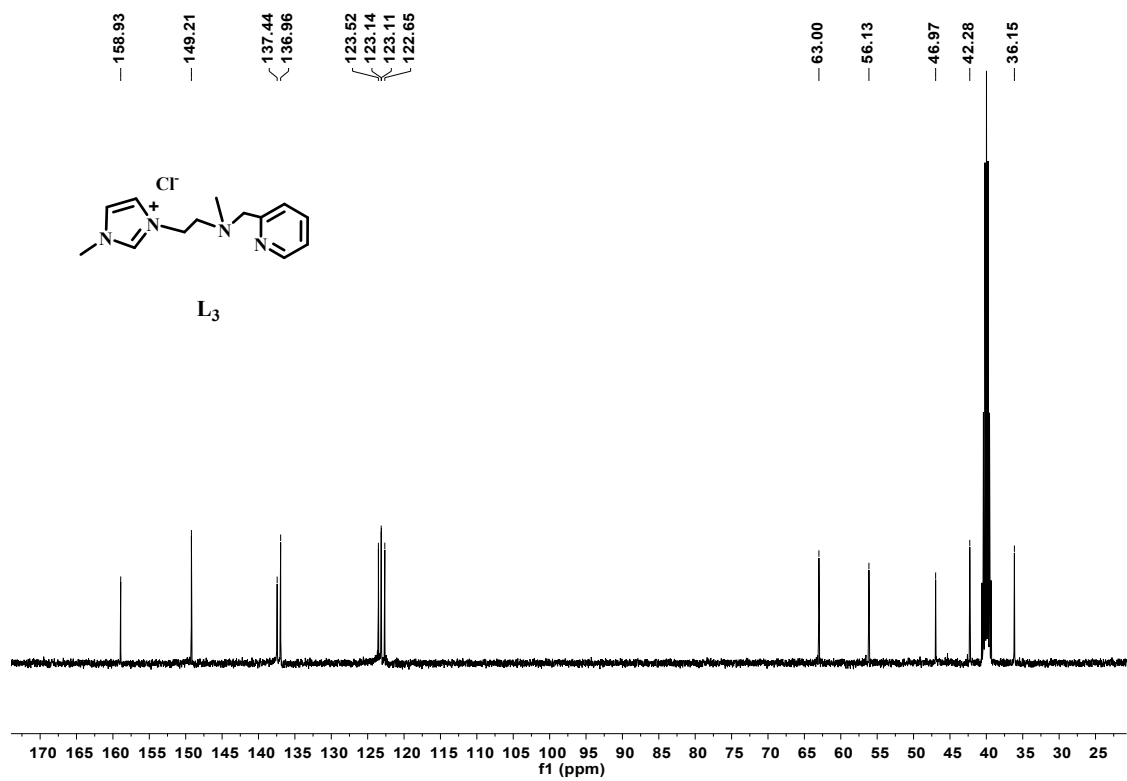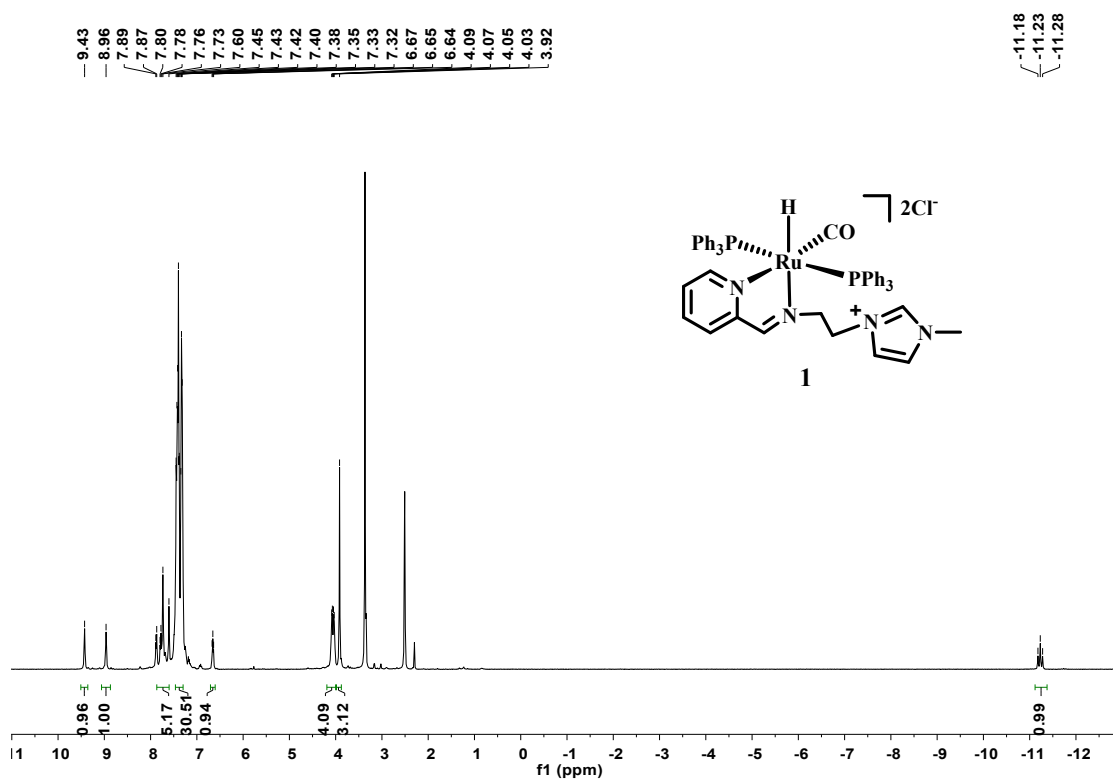
Figure S6. ¹³C NMR spectrum of **L3** (100 MHz, DMSO-*d₆*).

Figure S7. ¹H NMR spectrum of complex **1** (400 MHz, DMSO-*d₆*).

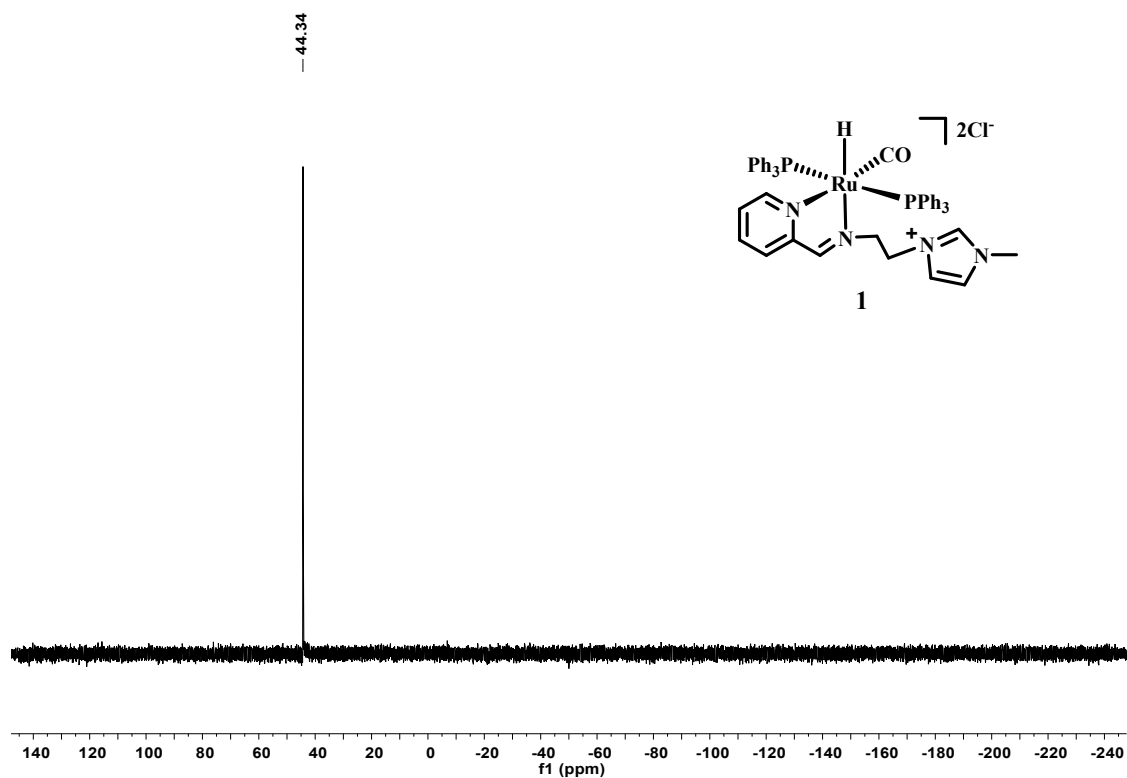**Figure S8**. $^{31}P\{^1H\}$ NMR spectrum of complex **1** (162 MHz, DMSO-d_6).

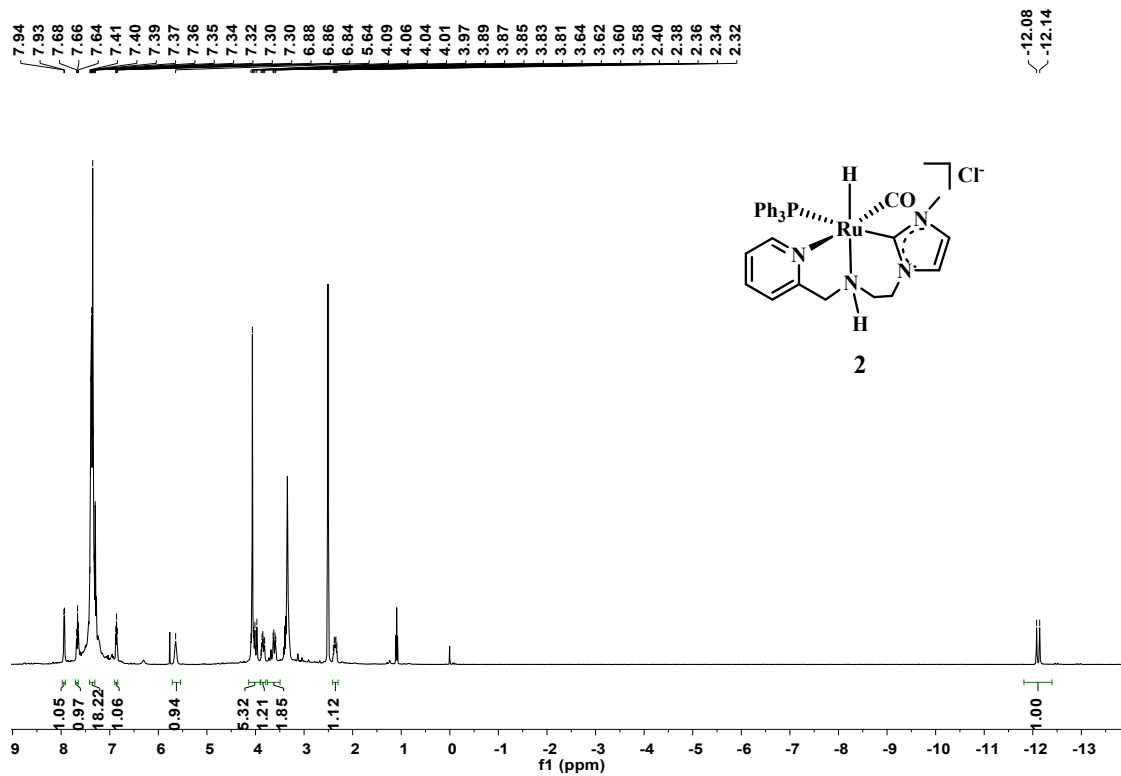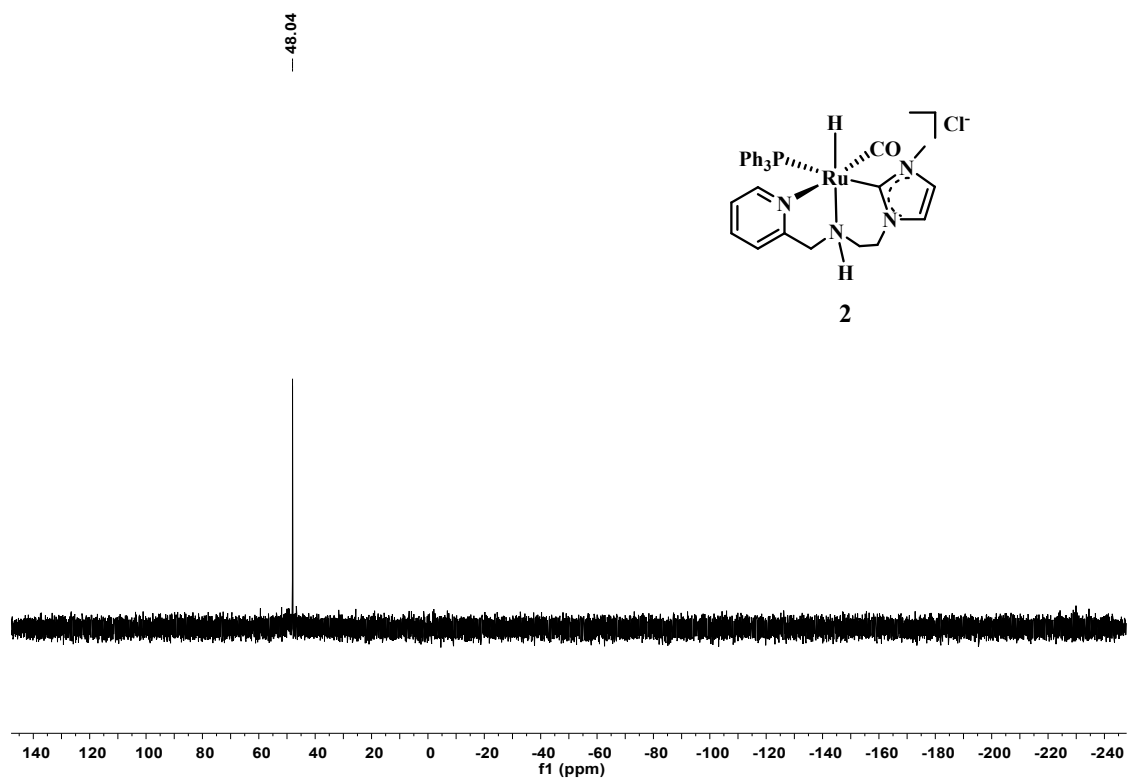**Figure S9**. ^1H NMR spectrum of complex **2** (400 MHz, DMSO-d_6).

Figure S10. $^{31}P\{^1H\}$ NMR spectrum of complex **2** (162 MHz, DMSO-d_6).

Figure S11. ^{13}C NMR spectrum of complex **2** (100 MHz, DMSO-d_6). Note: the two single peaks at 15.6 and 65.4 ppm are attributed to ether. Single peak at 55.4 ppm is attributed to dichloromethane.

Figure S12. ^{1}H NMR spectrum of complex **3** (400 MHz, DMSO-d_6).
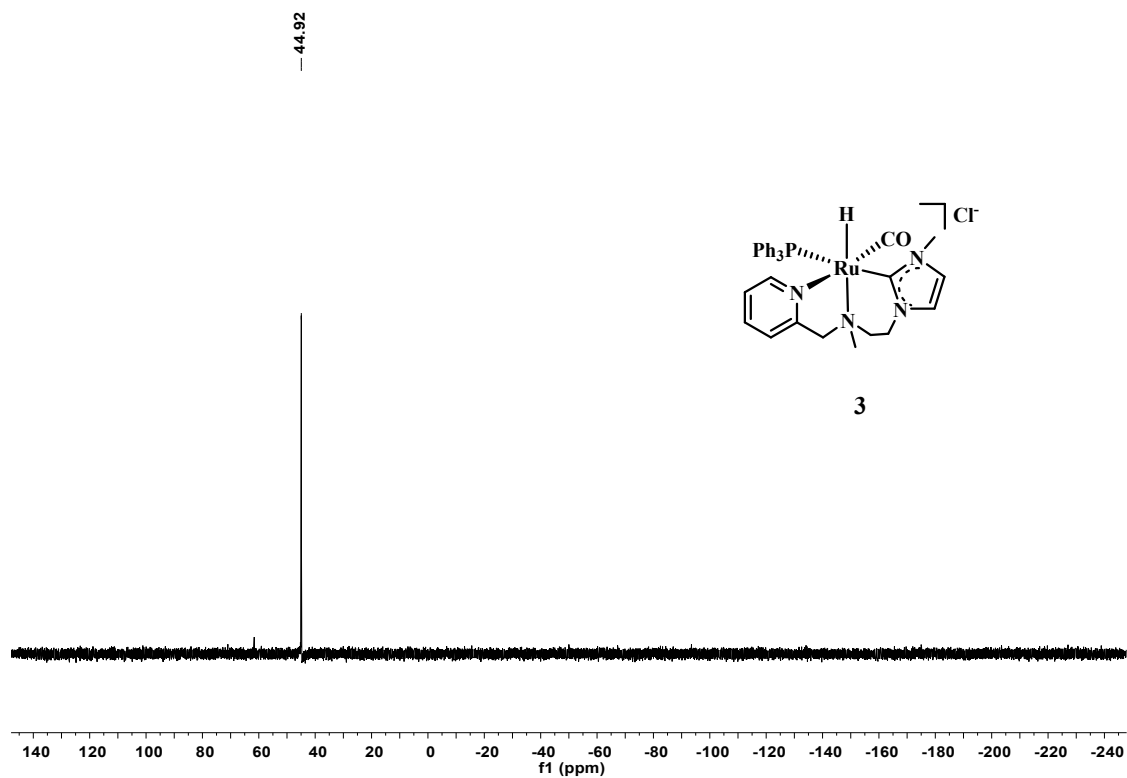
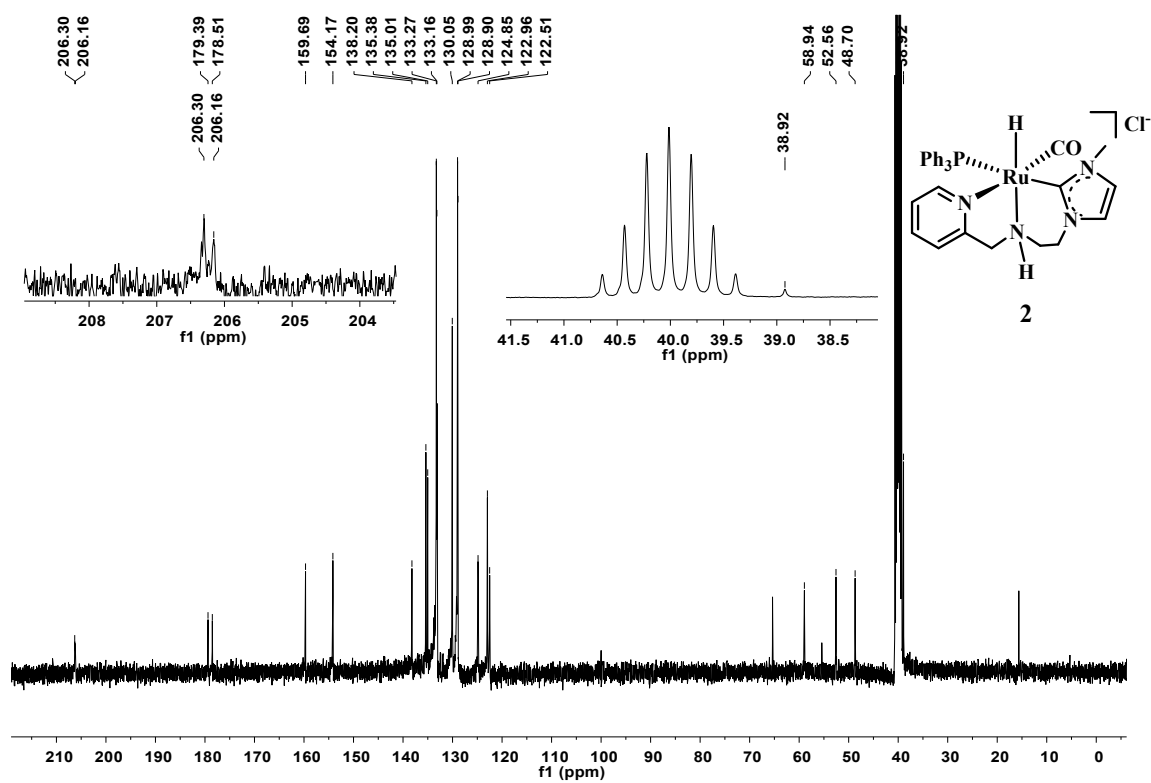**Figure S13**. ^{31}P{^{1}H} NMR spectrum of complex **3** (162 MHz, DMSO-d_6).
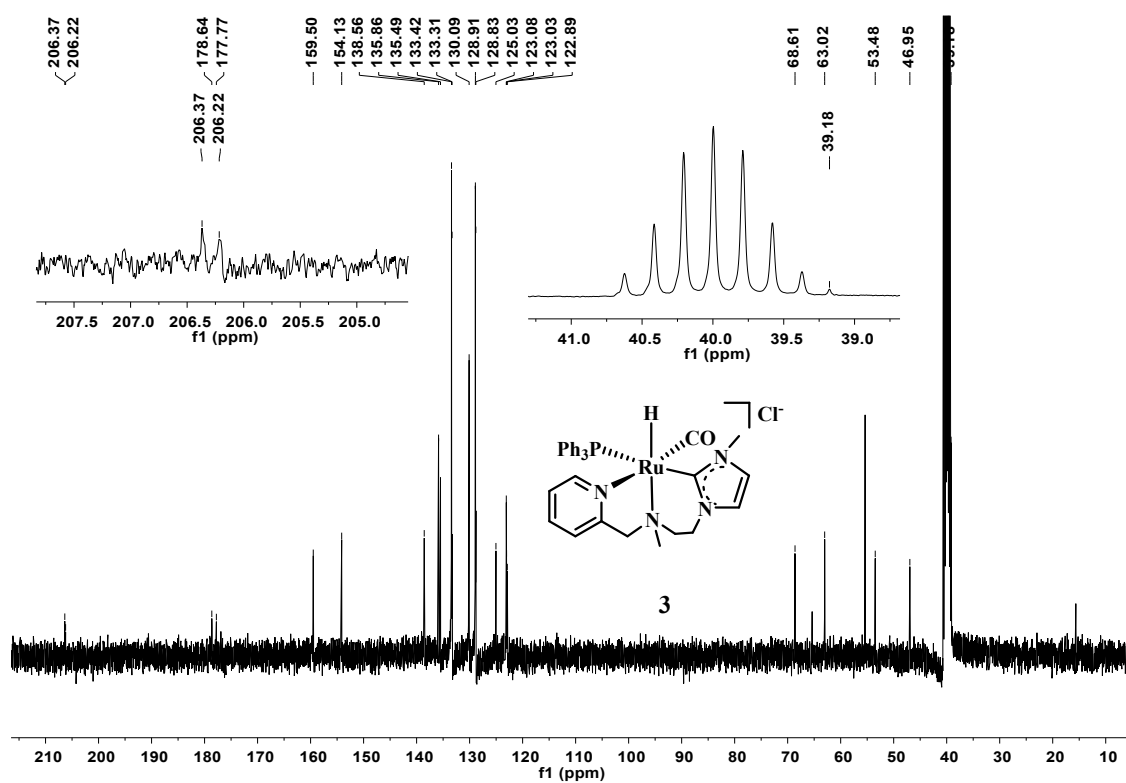
Figure S14. ^{13}C NMR spectrum of complex **3** (100 MHz, DMSO-d_6). Note: the two single peaks at 15.6 and 65.4 ppm are attributed to ether. Single peak at 55.4 ppm is attributed to dichloromethane.
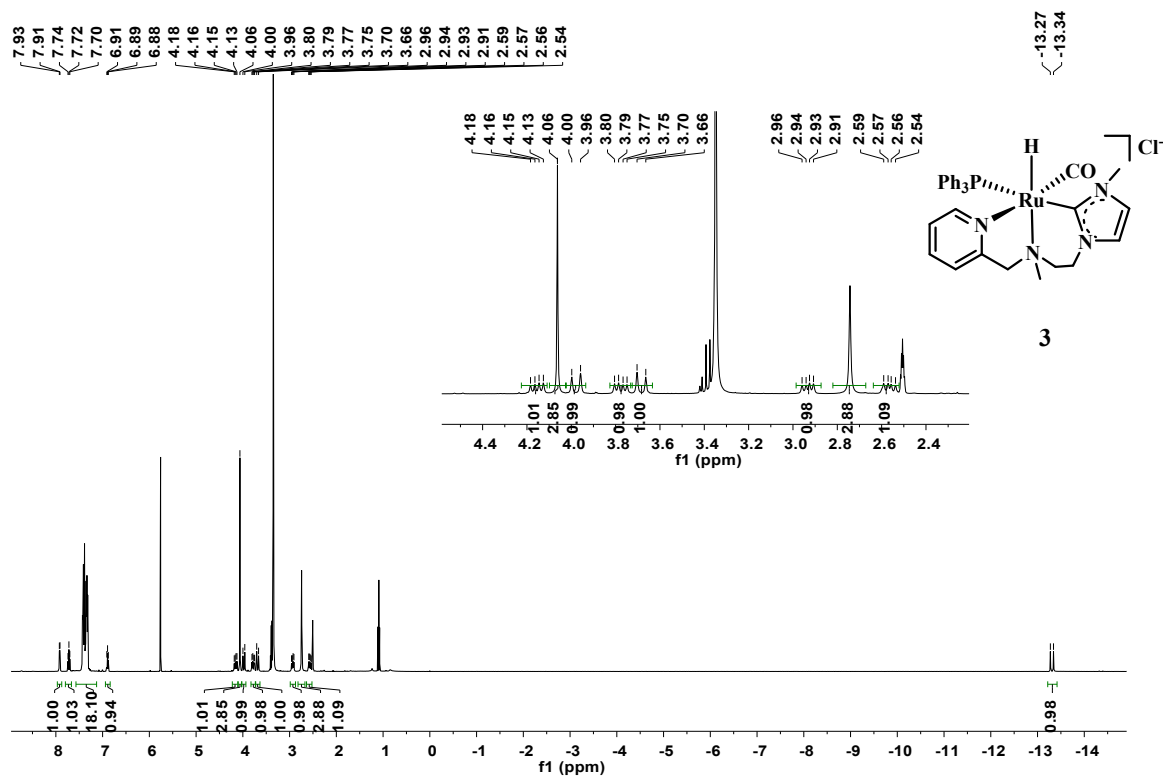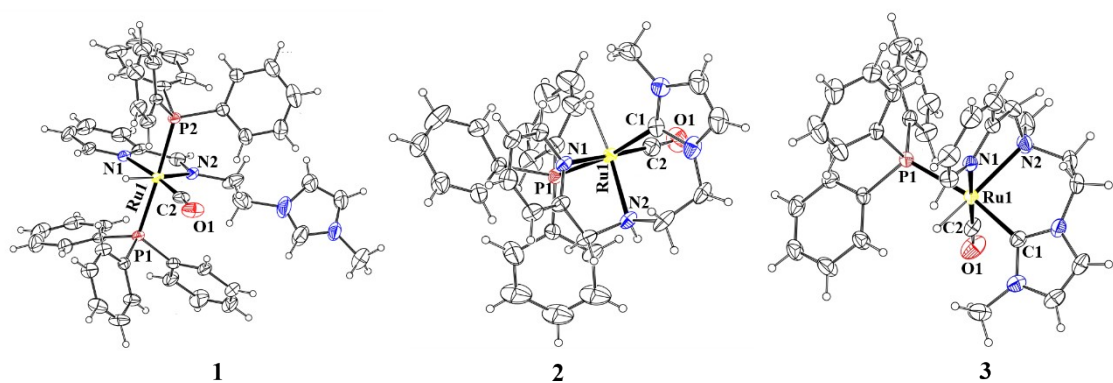

Figure S15. X-ray crystal structures of complexes **1** (BF$_4^-$), **2** and **3** (BF$_4^-$), the counterion is omitted (These structures are obtained from Reference[1], CCDC 2125582, 2125759 and 2125625 contain the supplementary crystallographic data for complexes **1-3**).

1.2 General procedure of transfer hydrogenation of CO_2.

Complex **1** was slightly soluble in water at room temperature, while complexes **2** and **3** were soluble in water at room temperature. A fresh stock solution of complex **1** or **2** or **3** was prepared prior to the experiment. For example, 40 μmol complex was dissolved in 100 mL degassed H_2O, and diluted to 0.02 μmol/mL with H_2O. The reactions were carried out in a Hastelloy Autoclave Reactor system equipped with a 50 mL cylinder. Under a nitrogen atmosphere, 5.0 mL of a stock solution of complex (0.02 μmol/mL, 0.1μmol), K_2CO_3 (24 mmol), glycerol or isopropanol (5.0 ml) were added to an autoclave. The autoclave was then sealed, pressurized with CO_2 and stirred at room temperature until the pressure of CO_2 no longer dropped, and the pressurized CO_2 was adjusted to the required pressure (10-50 bar). The mixture was vigorously stirred and heated at 110-200 ℃ for the desired time (5-100 h). Then, the reaction mixture was cooled down to ambient temperature, and diluted with H_2O. 100-500 μl of DMF (dimethylformamide) was added as internal standard, then, the amount of formate, acetate and lactate were quantified by ^{1}H NMR spectroscopy in D_2O. The residual hydrogen in gas phase after reaction is analyzed by gas chromatography. The reactions were run three times, and the average numbers of mmol were used.

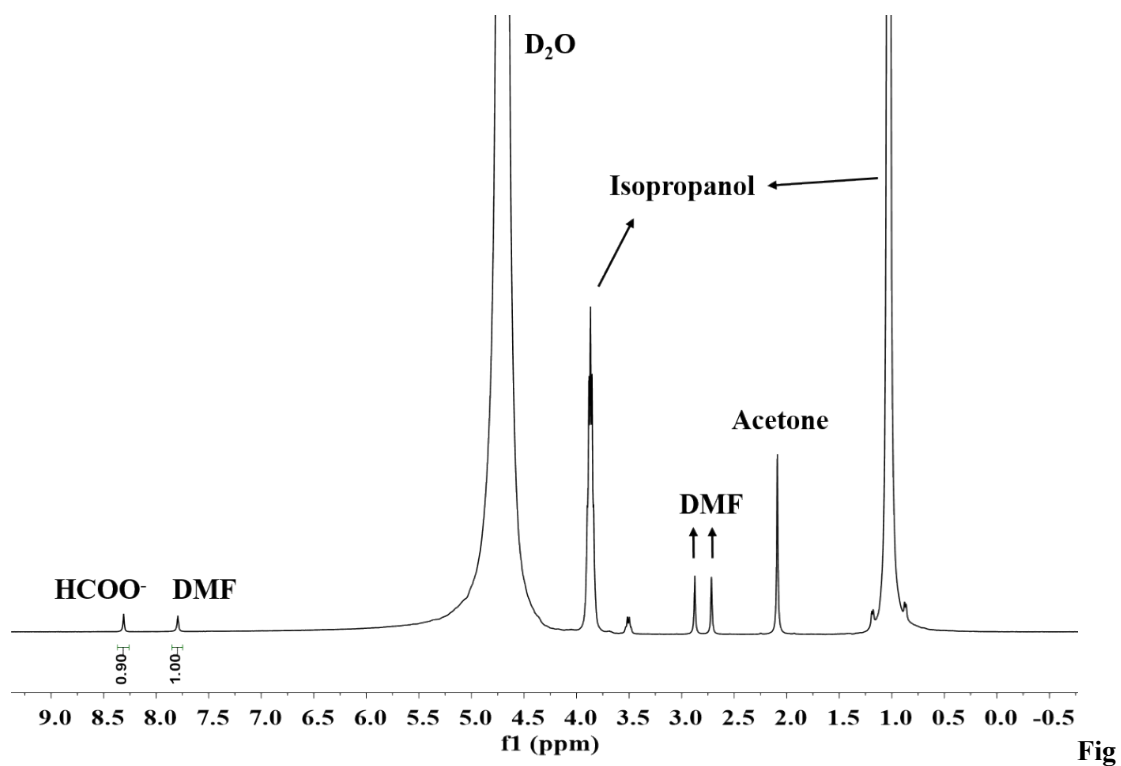**Representative ^{1}H NMR of the reaction mixtures**

ure S16. ^{1}H NMR spectrum of the reaction mixture performed with isopropanol using DMF as internal standard.
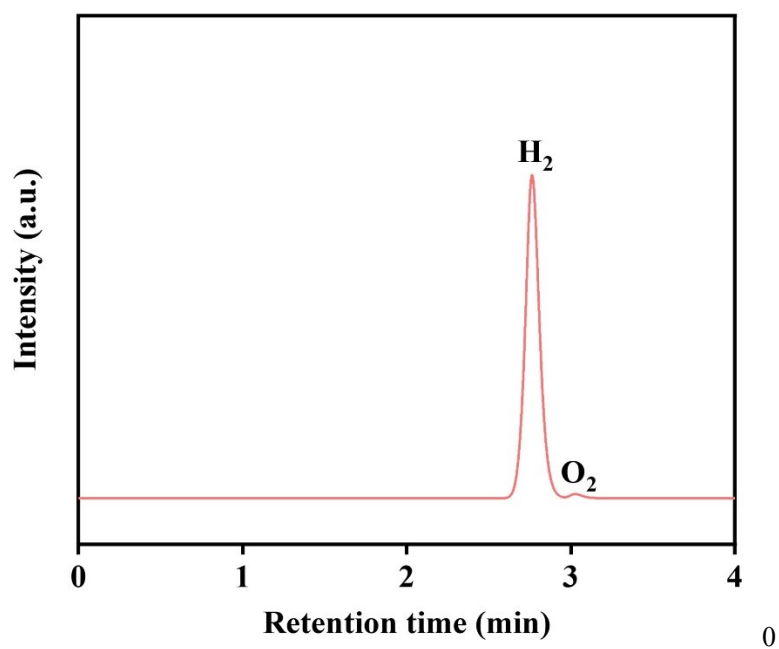

Figure S17. After reaction, hydrogen in gas phase was detected by gas chromatography.

2. Additional catalytic data

Table S1. Transfer hydrogenation of CO_2 to formate with ^{i}PrOH.

entry[a]	catalyst	base	HCOO⁻ (mmol)	TON (HCOO⁻)	Acetone (mmol)	TON (acetone)
1	**1**	KOH	0.802	80	1.154	115
2	**2**	KOH	1.823	182	2.526	253
3	**3**	KOH	0.388	39	0.37	37
4[b]	**2**	KOH	0	0	-	-
5[c]	**2**	KOH	0	0	4.252	425
6	**2**	/	0	0	0.431	43
7	**2**	NaOH	1.874	187	1.250	125
8	**2**	K_2CO_3	2.069	207	2.004	200
9	**2**	$KHCO_3$	1.771	177	2.922	292
10	**2**	Na_2CO_3	0.749	75	0.746	75
11	**2**	TEA	1.254	125	0.825	83
12	**2**	TEOA	0.504	50	1.121	112
13	**2**	DBU	0.685	69	1.312	131
14[d]	**2**	K_2CO_3	2.586	259	4.329	433
15[e]	**2**	K_2CO_3	3.090	309	4.911	491
16[f]	**2**	K_2CO_3	3.103	310	3.710	371
17[g]	**2**	K_2CO_3	2.444	244	3.903	390
18[h]	**2**	K_2CO_3	1.786	179	2.673	267

[a] Reaction conditions: 10 μmol complex, base (24 mmol), H_2O / ^{i}PrOH (5 mL/5 mL), 50 bar CO_2, T = 150 °C, t = 20 h. TEA = triethylamine; TEOA = triethanolamine; DBU = 1,8-diazabicyclo [5.4.0] undec-7-ene. [b] without ^{i}PrOH. [c] without CO_2. [d] 40 bar CO_2. [e] 20 bar CO_2. [f] 10 bar CO_2. [g] 1 bar CO_2. [h] base 12 mmol. Formate and acetone were quantified by ^{1}H NMR analysis in D_2O and using DMF as internal standard.

The effect of CO_2 pressure on the hydrogen-transfer reduction of CO_2 was evaluated (Table 2, entries 1-4). Interestingly, lower CO_2 pressure is favorable for CO_2 transfer hydrogenation, and the TON values of formate gradually decrease along with the raising of CO_2 pressure. We proposed two possible reasons for this phenomenon. It was reported that the transfer hydrogenation of CO_2 to formate favors basic media.[2, 3, 4] More CO_2 will dissolve in the solution due to the higher CO_2 pressure, which reduces the pH of the solution and is unfavorable for the transfer hydrogenation of CO_2.[3, 4] Moreover, the higher pressure is not beneficial for the formation of hydrogen

thermodynamically, and the suppressed dehydrogenation of ^{i}PrOH might also lead to the poor CO_2 transfer hydrogenation performance.

KOH, K_2CO_3, and $KHCO_3$ were all converted into HCO_3^- in an aqueous solution under high CO_2 pressure. Since K_2CO_3 yields 2 equivalents of HCO_3^-, it exhibits the strongest alkalinity when compared with an equal molar amount of KOH and $KHCO_3$ in the presence of excess CO_2, resulting in higher activity for K_2CO_3 (Table S1, entries 2, 8-9). When the same molar concentration of K^+ (12 mmol of K_2CO_3) was used, the $TON_{formate}$ in the K_2CO_3 aqueous solution was found to be similar to that in KOH or $KHCO_3$ (Table S1, entry 18).

Table S2. Effect of temperature on the transfer hydrogenation reaction

entry	T/°C	alcohol	$HCOO^-$		Acetone	
			(mmol)	TON	mmol	TON
1	110	^{i}PrOH	0.634	63	0.352	35
2	130	^{i}PrOH	1.694	169	0.799	80
3	150	^{i}PrOH	3.090	309	4.911	491
4	170	^{i}PrOH	4.060	406	6.25	625
5	200	^{i}PrOH	4.111	411	7.22	722

[a]Reaction conditions: 10 μmol complex **2**, K_2CO_3 (24 mmol), H_2O / ^{i}PrOH (5 mL/5 mL), 20 bar CO_2, t = 20 h.

Table S3. Influence of K_2CO_3 concentration on the activity of CO_2 transfer hydrogenation

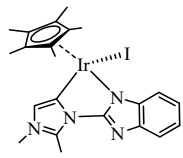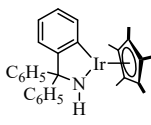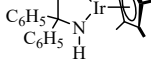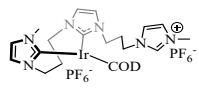| entry	alcohol	K_2CO_3 (mmol)	HCOOK (mmol)	TON (formate)	lactate	TON
					TON	
1	^{i}PrOH	6	0.607	607	-	
2	^{i}PrOH	12	1.073	1070	-	
3	^{i}PrOH	24	4.034	4030	-	
4	Glycerol	6	1.177	1180	2663	185
5	Glycerol	12	1.616	1620	2728	193
6	Glycerol	24	3.391	3390	6460	228
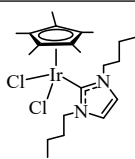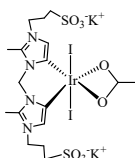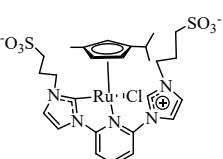
Reaction conditions: 1 μmol complex **2**, K_2CO_3 (6-24 mmol), H_2O / ^{i}PrOH or Glycerol (5 mL/5 mL), 20 bar CO_2, T = 170 °C, t = 20 h.

Table S4. Effect of catalyst amounts on catalytic CO_2 transfer hydrogenation with ^{i}PrOH

entry	Cat./ μmol	T/°C	Time (h)	HCOOK (mmol)	TON	^{i}PrOH conv. %	Acetone	
							mmol	TON
1	10	170	20	4.060	406	22.5	6.25	625
2	5	170	20	3.930	786	21.7	4.71	943
3	1	170	20	4.034	4030	36.3	2.20	2200
4	0.5	170	20	3.775	7550	48.2	1.51	3017
5	0.1	170	20	1.162	11600	13.3	0.41	4100
6	0.1	170	50	1.526	15300	39.0	0.59	5900
7	0.1	170	100	2.590	25900	54.5	0.73	7327

Reaction conditions: complex **2**, K_2CO_3 (24 mmol), H_2O / ^{i}PrOH (5 mL/5 mL), 20 bar CO_2.

Table S5. Previously reported catalysts for the transfer hydrogenation of CO_2 and inorganic carbonates

Cat.	C1 Source	hydrogen donor	T (°C)	Time (h)	TON (formate)	TON (lactate)	Ref.
	CO_2 (50 bar)	^{i}PrOH	110	72	150	-	[5]
	CO_2 (50 bar)	^{i}PrOH	200	75	2700	-	[6]
	CO_2 (26 bar)	glycerol	180	24	1065	1685	[7]
	CO_2 (1 bar)	glycerol	150	12	1080	-	[8]
	CsHCO$_3$	^{i}PrOH	80	5	3200	-	[9]
	CO_2 (1 bar)	^{i}PrOH	80	5	655	-	
	CO_2 (5 bar)	glycerol	200	20	200 000	875 000	[10]
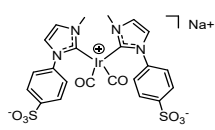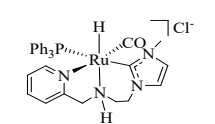
	K$_2$CO$_3$	glycerol	150	6	13350	27850	[11]
	CO$_2$ (20 bar)	glycerol	200	50	300000	387000	this work

Table S6. Independent glycerol dehydrogenation or CO$_2$ hydrogenation reactions.

entry	Cat. /μmol	T/°C	Time (h)	TON (FA)	TON (LA)	TON (AA)	P(H$_2$) /MPa
1[a]	0.1	200	20	15400	164000	11250	
2[b]	0.1	150	5	1720			1.0
3[b]	0.1	150	5	2840			2.0
4[b]	0.1	150	5	4030			3.0
5[b]	0.1	150	5	trace			0.1
6[b]	0.1	200	20	13100			1.0
7[c]	0.1	200	20	118000	176000	8620	

[a] Independent glycerol dehydrogenation without CO$_2$. [b] Independent CO$_2$ hydrogenation without glycerol. [c] Co-upcycling of glycerol and CO$_2$. FA: formate; LA: lactate; AA: acetate.
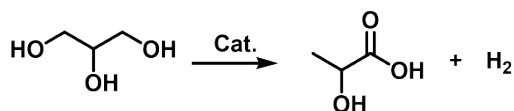
$$\text{Eq. 1}$$

$$pV = nRT \qquad \text{Eq. 2}$$

The Ru complex **2** can realize the dehydrogenation of glycerol into lactate and H$_2$ in the absence of CO$_2$ (Table S6, entry 1). Meanwhile, when glycerol was replaced by H$_2$, Ru complex **2** was also able to achieve the hydrogenation of CO$_2$ into formate (Table S6, entries 2-6), with the reaction rate increasing as H$_2$ pressure increases. Therefore, these two reactions can occur independently. However, we also found that CO$_2$ hydrogenation was difficult under low H$_2$ pressure (Table S6, entries 5-6). The theoretical H$_2$ yield (Eq. 1; Table S6, entry 1) is 0.0164 mol, corresponding to an H$_2$ partial pressure of 0.81 MPa (Eq. 2) in our system. To verify this, we measured the pressure of H$_2$ after the reaction and found that the partial pressure of H$_2$ was less than 1 MPa, which is disadvantageous for the hydrogenation of CO$_2$. Therefore, we assume that the active Ru-H intermediate formed during the dehydrogenation of glycerol could directly realize the hydrogenation of CO$_2$ to formate, without the need to generate free H$_2$ in advance (Figure S19, Table S6, entry 7). In this case, the dehydrogenation of glycerol would influence the subsequent CO$_2$ hydrogenation. However, it almost impossible to distinguish between the contributions of the Ru-H pathway and

the free H_2 pathway, as the hydrogenation of CO_2 with H_2 could also form the Ru-H intermediate (Figure S19).

Therefore, we prefer not to mention whether glycerol dehydrogenation and CO_2 hydrogenation are independent processes. Instead, we only emphasize that the Ru complex **2** can serve as the bifunctional catalysts for converting CO_2 and glycerol into formate and lactate simultaneously.

Computational methods of DFT

Gaussian 09[12] calculations were performed with the b3lyp density functional using a def2-SVP basis[13,14]. The Gibbs free energies, were calculated at T = 473.15 K and 1 atm pressure by Shermo[15]. The solvation effect of H_2O was included by performing single-point energy calculations using the SMD solvation model.
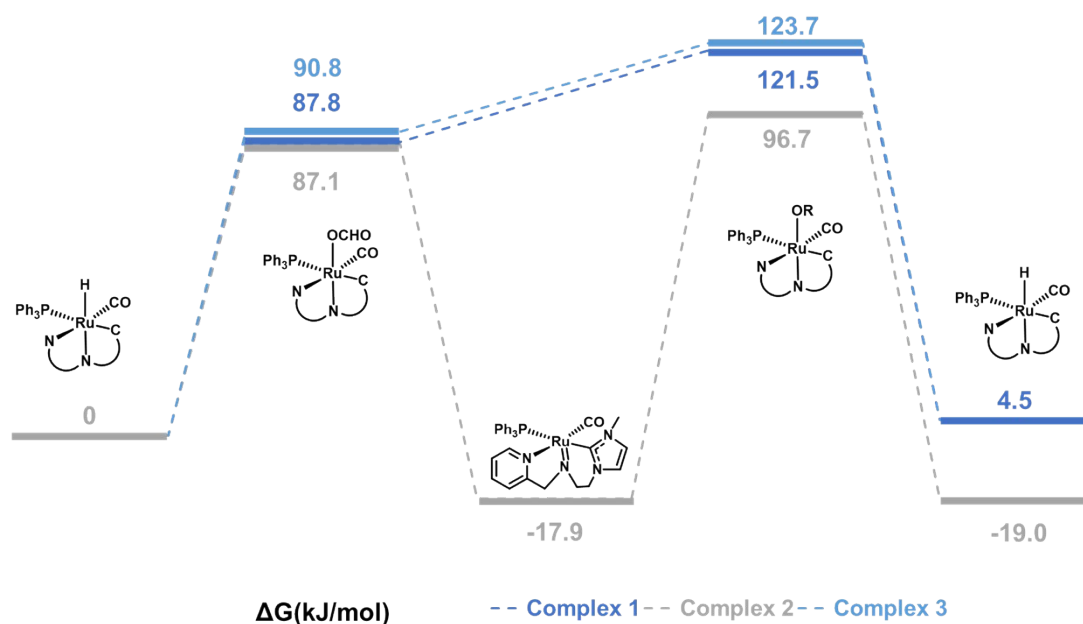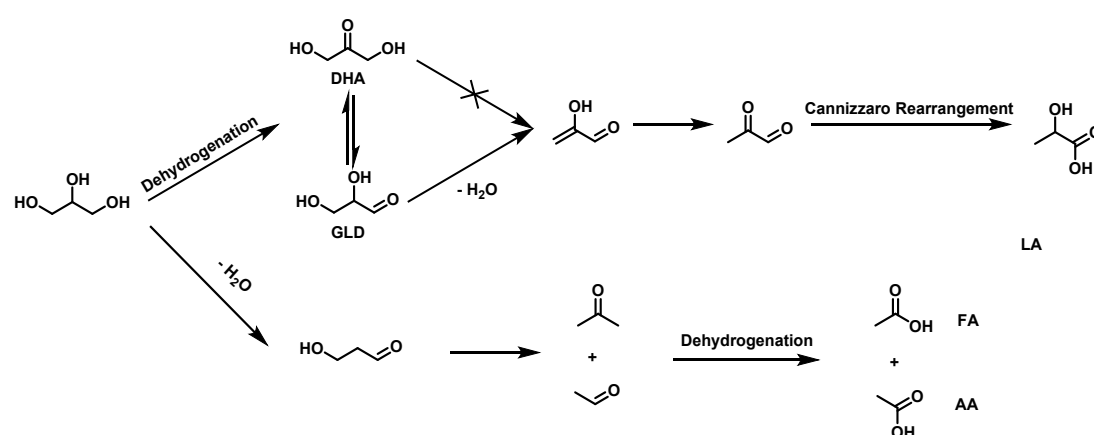

Figure S18. Gibbs free energy profiles at reaction temperature of complex **1-3**.

Scheme S3. Pathway for glycerol conversion[16-19]

As shown in Scheme N3 and further supported by isotope labeling experiments (Figure 2B), it is suggested that the conversion of glycerol is quite complex, and a small portion of the formate should

also originate from the C-C bond cleavages of glycerol rather than from CO_2 remaining in the water.
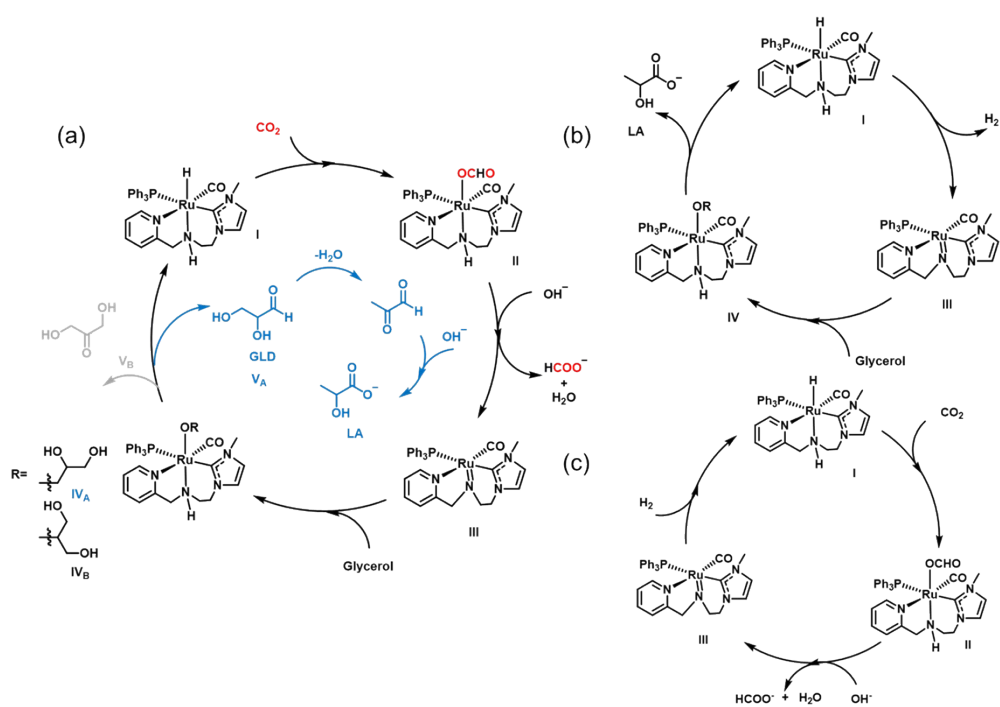

Figure S19. (a) Proposed catalytic cycle for the co-upcycling of CO_2 and glycerol. (b) Proposed catalytic cycle for independent glycerol dehydrogenation and (c) independent CO_2 hydrogenation.

References

1   H. H. Gong, T. H. Cui, Z. Y. Liu, Y. L. Zheng, X. L. Zheng, H. Y. Fu, M. L. Yuan, H. Chen, J. Q. Xu, R. X. Li, *Catal. Sci. Technol.*, 2022, **12**, 6213-6218.

2   Y. J. Cheong, K. Sung, S. Park, J. Jung and H. Y. Jang, *ACS Sustainable Chem. Eng.*, 2020, **8**, 6972-6978.

3   J. M. Heltzel, M. Finn, D. Ainembabazi, K. Wang and A. M. Voutchkova-Kostal, *Chem. Commun.*, 2018, **54**, 6184-6187.

4   Y. J. Cheong, K. Sung, J. A. Kim, Y. K. Kim, W. Yoon, H. Yun and H. Y. Jang, *Catalysts*, 2021, **11**, 695.

5   S. Sanz, M. Benítez and E. Peris, *Organometallics*, 2010, **29**, 275-277.

6   A. Azua, S. Sanz and E. Peris, *Chem. Eur. J.*, 2011, **17**, 3963-3967.

7   J. M. Heltzel, M. Finn, D. Ainembabazi, K. Wang and A. M. Voutchkova-Kostal, *Chem. Commun.*, 2018, **54**, 6184-6187.

8   A. Kumar, S. Semwal and J. Choudhury, *ACS Catal.*, 2019, **9**, 2164-2168.

9   Y. Sato, Y. Kayaki and T. Ikariya, *Chem. Commun.*, 2020, **56**, 10762-10765.

10   Y. J. Cheong, K. Sung, J. A. Kim, Y. K. Kim, W. Yoon, H. Yun and H. Y. Jang, *Catalysts*, 2021, **11**, 695.

11   D. Ainembabazi, K. Wang, M. Finn, J. Ridenour and A. Voutchkova-Kostal, *Green Chem.*, 2020, **22**, 6093-6104.

12   M. J. Frisch, G. W. Trucks, H. B. Schlegel, G. E. Scuseria, M. A. Robb, J. R. Cheeseman, G. Scalmani, V. Barone, G. A. Petersson, H. Nakatsuji, X. Li, M. Caricato, A. Marenich, J. Bloino, B. G. Janesko, R. Gomperts, B. Mennucci, H. P. Hratchian, J. V. Ortiz, A. F. Izmaylov, J. L. Sonnenberg, D. Williams-Young, F. Ding, F. Lipparini, F. Egidi, J. Goings, B. Peng, A. Petrone, T. Henderson, D. Ranasinghe, V. G. Zakrzewski, J. Gao, N. Rega, G. Zheng, W. Liang, M. Hada, M. Ehara, K. Toyota, R. Fukuda, J. Hasegawa, M. Ishida, T. Nakajima, Y. Honda, O. Kitao, H. Nakai, T. Vreven, K. Throssell, J. A. Montgomery, Jr., J. E. Peralta, F. Ogliaro, M. Bearpark, J. J. Heyd, E. Brothers, K. N. Kudin, V. N. Staroverov, T. Keith, R. Kobayashi, J. Normand, K. Raghavachari, A. Rendell, J. C. Burant, S. S. Iyengar, J. Tomasi, M. Cossi, J. M. Millam, M. Klene, C. Adamo, R. Cammi, J. W. Ochterski, R. L. Martin, K. Morokuma, O. Farkas, J. B. Foresman, and D. J. Fox, Gaussian, Inc., Wallingford CT, 2016.

13   F. Weigend, *Phys. Chem. Chem. Phys.*, 2006, **8**, 1057–1065.

14   F. Weigend and R. Ahlrichs, *Phys. Chem. Chem. Phys.*, 2005, **7**, 3297–3305.

15   T. Lu and Q. Chen, *Comput. Theor. Chem.*, 2021, **1200**, 113249.

16   M. Tao, Dan Zhang, H. Guan, G. Huang and X. Wang, *Sci. Rep.*, 2016, **6**, 29840.

17   G. Y. Yang, Y. H. Ke, H. F. Ren, C. L. Liu, R. Z. Yang and W. S. Dong, *Chem. Eng. J.*, 2016, **283**, 759-767.

18   L. S. Sharninghausen, J. Campos, M. G. Manas and R. H. Crabtree, *Nat. Commun.*, 2014, **5**, 5084.

19   J. Wu, X. Liu, Y. Hao, S. Wang, R. Wang, W. Du, S. Cha, X.-Y. Ma, X. Yang and M. Gong, *Angew. Chem. Int. Ed.*, 2023, **62**, e202216083.